A Synchronization Method for Grid Converters with Enhanced Small-Signal and Transient Dynamics

Steinkohl, Joachim; Taul, Mads Graungaard; Wang, Xiongfei; Blaabjerg, Frede; Hasler, Jean-Philippe

Published in:
Proceedings of 2018 IEEE 19th Workshop on Control and Modeling for Power Electronics (COMPEL)

DOI (link to publication from Publisher):
10.1109/COMPEL.2018.8460113

Publication date:
2018

Document Version
Accepted author manuscript, peer reviewed version

A Synchronization Method for Grid Converters with Enhanced Small-Signal and Transient Dynamics

J. Steinkohl*, M. G. Taul†, X. Wang‡ and F. Blaabjerg§
Department of Energy Technology
Aalborg University
Aalborg, Denmark
*joa@et.aau.dk, †mkg@et.aau.dk, ‡xwa@et.aau.dk, §fbl@et.aau.dk

J. -P. Hasler
ABB FACTS
Västerås, Sweden
jean-philippe.hasler@se.abb.com

***Abstract*—An increasing integration of voltage source based renewable energy systems into the power system is a global trend, that has led to requirements for converter control during low voltage and fault situations. To guarantee stable operation, grid synchronization is a key factor, which greatly influences the stability and ride-through performance of the converter. This paper proposes an improved grid synchronization technique, which enhances the transient performance of the converter under severe grid conditions, such as three phase faults and voltage phase jumps. This is achieved by combining a low bandwidth Synchronous Reference Frame Phase-Locked Loop (SRF-PLL) together with a feed-forward term. This combination effectively results in a synchronization unit including high noise immunity, e.g. enhanced small-signal performance and a fast dynamic response with a phase tracking capability below 5 ms. The proposed synchronization unit is tested during phase jumps and symmetrical three-phase faults to analyze its performance, which is validated through simulations and experimental results.**

***Index Terms*—Grid Connected Converter, Fault Ride Through, Grid Synchronization, Phase-Locked-Loop**

I. Introduction

Due to an increasing penetration of renewables into the power system, Transmission System Operators (TSOs) have issued grid codes requiring e.g. wind farms to stay connected during fault events and perform voltage support through reactive current injection [1], [2]. For proper fault performance, the grid-side converter of e.g. a wind turbine or Photo-Voltaic power conversion system must be able to control its injected current in a fast and accurate manner. However, a fast inner current loop in a vector controlled converter will not alone be responsible for such behavior, since its reference generation is determined by the synchronization unit of the converter, often a Synchronous Reference Frame Phase-Locked Loop (SRF-PLL) [3]–[5]. Extensive studies have been conducted for the SRF-PLL to investigate its influence on controller performance and converter stability [6]. To avoid coupling between the current controller and the outer synchronization loop, which decreases the small-signal stability, seen as frequency oscillations, the SRF-PLL is often tuned with a low bandwidth to achieve a high noise immunity.

Furthermore, the SRF-PLL is reported to be destabilized during weak grid conditions and fault events [7]–[9]. Several approaches have been proposed to keep a stable and slow SRF-PLL, while being able to inject desired currents during low-voltage ride-through conditions. These include freezing the SRF-PLL or setting the bandwidth low enough such that the SRF-PLL essentially is not aware of the fault event. In such a way, the frequency and angle estimation remains constant and the current controller can quickly inject reactive current into the grid to support the voltage. However, in case of any phase jumps during a fault, these two methods will completely change the performance of the system and will make it difficult to comply with grid code requirements. Firstly, when entering a fault, full reactive current should be injected within 20 ms [10], which implies that a fast synchronization method must be utilized to achieve this.

Secondly, during fault recovery, wind turbines or PV plants must quickly switch back to supply the loads of the system. Considering a slow SRF-PLL and phase jumps in the grid voltage during fault recovery, the converter system will inject reactive power into a healthy network leading to overvoltages, which is highly undesired. Thus, during severe grid conditions, a fast SRF-PLL scheme is needed [11].

In [4], a comprehensive review of a large number of studies regarding different SRF-PLL-enhancements are presented. Since the difference mainly lies in the way the phase detection is performed, i.e. advanced pre-filtering techniques, most available SRF-PLL structures are not able to achieve a dynamic response faster than 20 ms. One exception could be a type-1 PLL, which only utilizes one integrator by eliminating the internal PI controller. This controller possess fast dynamic behaviour but is unable to track the grid during any frequency drifts due to the elimination of the PI controller [12]. Instead of attenuating unwanted effects from the input using filters, which decrease the dynamic performance, a delayed signal cancellation method can be used, which block certain signals rather than attenuating them [13]. This unfortunately shares the disadvantage as for type-1 PLLs, which is a deteriorated response if the grid frequency drifts from the nominal value.

In [11], a hybrid SRF-PLL is proposed which in case of a transient event switches to a fuzzy logic controller, which is able to synchronize to the grid within 5 ms. This method, however, requires logic to decide when to use the

fuzzy controller due to its oscillating response under normal operation and it is a rather complex controller to implement, which is not likely to be adopted by industry. To mitigate the aforementioned limitations, this paper presents a fast and simple converter synchronization method, possessing robust steady-state performance while being able to track transient events with a high bandwidth and precision. This is achieved by utilizing a structure based on a SRF-PLL together with a ideal angle estimation, which can be designed to achieve a desired dynamic performance.

The paper is organized as follows. A description of the existing SRF-PLL synchronization method is presented in Section II and a description of the proposed controller is Section III. Analysis of the method together with simulation results are presented in Section IV-A, which is experimentally validated in Section IV-B. Finally, Section V summarizes the conclusions of the paper.

II. SRF-PLL

The SRF-PLL is a control algorithm used to extract the angle θ_{G} of the grid voltage vector in order to construct a desired current reference value in a grid connected power converter. This is done, by using the Park-Transformation with the estimated angle of the grid from the SRF-PLL [14]. The mathematical representation for V_d and V_q are given by (1) and (2).

$$V_{\mathrm{d}} = |V_{\mathrm{G}}| \cdot \cos\left(\theta_{\mathrm{G}} - \theta_{\mathrm{PLL}}\right) \tag{1}$$

and

$$V_{\mathrm{q}} = |V_{\mathrm{G}}| \cdot \sin\left(\theta_{\mathrm{G}} - \theta_{\mathrm{PLL}}\right) \tag{2}$$

The synchronization is done, by controlling the q-axis voltage component to zero, as shown in Fig. 1. Any deviation in V_q from zero is corrected by the PI controller by adjusting the internal frequency estimation, which is then integrated in order to obtain the synchronous angle θ_{PLL}.

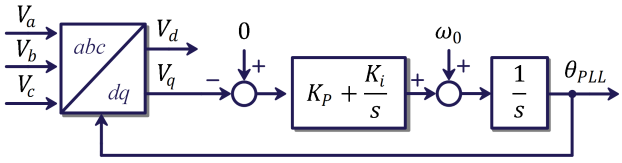

Fig. 1. Conventional structure of SRF-PLL.

As shown in (2), V_q is dependent on the voltage magnitude as well. To compensate this, it can be normalized with the voltage magnitude to get a value, that is only relying on the phase difference, as in [15]. This normalization leads then to

$$V_{\mathrm{q\ norm}} = \frac{V_{\mathrm{q}}}{|V_{\mathrm{G}}|} = \sin\left(\theta_{\mathrm{G}} - \theta_{\mathrm{PLL}}\right) \tag{3}$$

In (3), the angle difference is small under steady-state-condition. So the small angle simplification can be used, where the sinus of the small angle signal ($\theta_{\mathrm{G}} - \theta_{\mathrm{PLL}}$) is the angle difference itself. But this is still a simplification, that is only valid for small angle disturbances.

Due to the fact, that the SRF-PLL is normally tuned with a low bandwidth to avoid instability issues and coupling effects with the current controller, the dynamic performance and tracking capability of the synchronization unit is inherently slow. This is not allowed under transient conditions, in the case of grid faults, where the phase can change rapidly.

III. Proposed controller

The controller will combine the advantages of the SRF-PLL with the dynamic feed-forward of the error angle information, that can be calculated from V_q and V_d as described in [16]. This allows, to control not the value V_q, that is dependent on the voltage magnitude and the phase, but directly the phase. The control diagram can be seen in Fig. 2.

The controller feeds the error signal of the angle deviation forward to the output angle signal. This feed-forward does not have a direct impact on the inner control loop to the SRF-PLL dynamics as it is proposed in [17]. The impact of the current output to the voltage of the grid is still remaining, especially under low voltage conditions. This control structure leads to two significant improvements.

First, the SRF-PLL is now not only linearized around small angles, but the input of the PI controller is inherently the angle difference, that has to be controlled to zero. Second, this angle difference is not a sinusoidal signal, but a DC signal. This allows further control that are not recommended for periodic signals. By making a feed-forward signal as shown in Fig. 2 allows to get a faster response to transient events, without changing the internal dynamics of the SRF-PLL. In the feed-forward, there can be low-pass filters (LPF) or other additional logic.

The angle information for the current control loop is shown in (4). The proposed synchronization allows to decouple the steady state frequency-dependent change rate of the angle and the transient event angle deviation. By controlling the feed-forward, is it now possible to control directly the dynamics under transient events.

$$\theta_{\mathrm{OUT}} = \theta_{\mathrm{PLL}} + FF \cdot \left(\theta_{\mathrm{G}} - \theta_{\mathrm{PLL}}\right) \tag{4}$$

The feed-forward block can include a wide range of control functionality, e.g. a low-pass filter which can be optimized to entail a desired performance.

A. Analysis

The transfer function of the PI controller in the SRF-PLL can be written as

$$G_{PI}(s) = K_p + K_i \cdot \frac{1}{s} \tag{5}$$

The open-loop and closed-loop transfer function of the linear SRF-PLL without the proposed feed-forward technique are

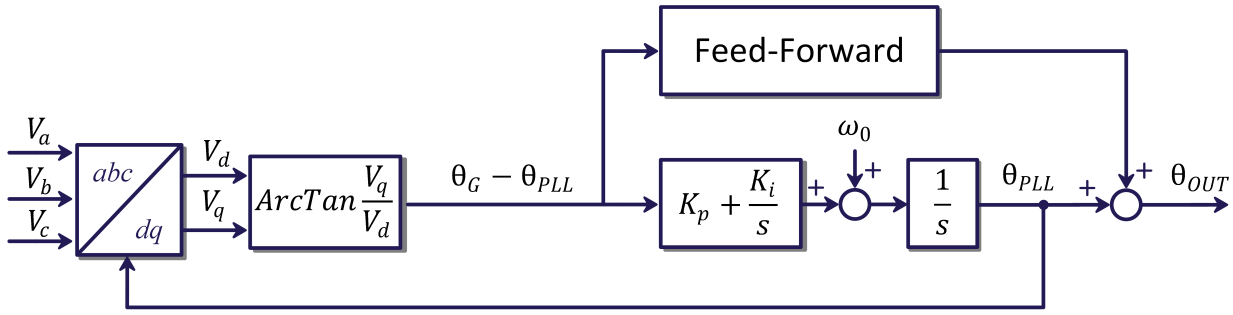

Fig. 2. Proposed structure of SRF-PLL with feed-forward.

$$G_{ol}(s) = G_{PI}(s) \cdot \frac{1}{s} \tag{6}$$

and

$$G_{cl}(s) = \frac{G_{PI}(s) \cdot \frac{1}{s}}{1 + G_{PI}(s) \cdot \frac{1}{s}} \tag{7}$$

To analyze the system with feed-forward, the steady state model has been developed. It is shown in Fig. 3.

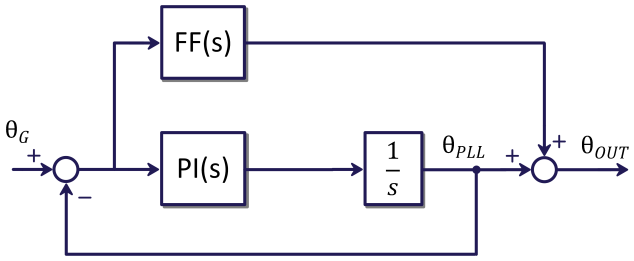

Fig. 3. Small signal model of the linear SRF-PLL with feed-forward control.

Considering the effect of the feed-forward path, the output estimated phase angle is

$$\theta_{OUT}(s) = (\theta_G(s) - \theta_{PLL}(s)) \cdot \left(G_{PI}(s) \cdot \frac{1}{s} + FF(s) \right) \tag{8}$$

where $G_{PI}(s)$ is the transfer function of the internal PI controller of the SRF-PLL and $FF(s)$ is a linear block that represents the feed-forward transfer function. θ_{OUT} can be expressed as

$$\theta_{OUT}(s) = \theta_{PLL}(s) \left(1 + \frac{FF(s)}{G_{PI}(s) \cdot \frac{1}{s}} \right) \tag{9}$$

This allows the elimination of θ_{PLL} in (8) and the closed-loop relationship between the phase angle of the grid voltage and the estimated output phase angle is

$$G_{cl,FF}(s) = \frac{\theta_{OUT}(s)}{\theta_G(s)} = \frac{G_{PI}(s) \cdot \frac{1}{s} + FF(s)}{1 + G_{PI}(s) \cdot \frac{1}{s}} \tag{10}$$

which has the open-loop transfer function

$$G_{ol,FF}(s) = \frac{FF(s) + G_{PI}(s) \cdot \frac{1}{s}}{1 - FF(s)} \tag{11}$$

Realizing the feed-forward path as a first order low-pass filter,

$$FF(s) = \frac{\alpha_F}{\alpha_F + s} \tag{12}$$

the expanded open-loop and closed-loop transfer function for the proposed synchronization unit becomes

$$G_{ol,FF}(s) = \frac{(K_p + \alpha_F)s^2 + (K_p\alpha_F + K_i)s + K_i\alpha_F}{s^3} \tag{13}$$

and

$$G_{cl,FF}(s) = \frac{(K_p + \alpha_F)s^2 + (K_p\,\alpha_F + K_i)s + K_i\,\alpha_F}{s^3 + (K_p + \alpha_F)s^2 + (K_p\,\alpha_F + K_i)s + K_i\,\alpha_F} \tag{14}$$

As it can be seen if $\alpha_F = 0$, the original closed-loop transfer function shown in (7) is obtained as expected from (14). By neglecting the inner current loop and the coupling between the injected current and the PCC voltage, the open-loop transfer functions and, hence, the dynamics of the linear SRF-PLL and linear SRF-PLL including feed-forward are different. By only looking at the characteristic equation, the SRF-PLL will always have complex conjugated poles in the left-half plane if $K_p > 0$ and $K_i > K_p^2/4$. Likewise by including a low-pass filter in the feed-forward path, the system will be stable with a complex conjugated pole pair and a real pole in the left-half plane if the same conditions are meet and provided that the bandwidth of the low-pass filter is positive, which is always true. Therefore, seen from the analysis of characteristic equations and Routh-Hurwitz stability criterion, the proposed feed-forward control does not change the stability. Actually, the poles of the characteristic equation of (14) is

$$p_1 = -\alpha_F \tag{15}$$

$$p_{2,3} = \frac{-K_p \pm \sqrt{K_p^2 - 4K_i}}{2} \tag{16}$$

This means that the two poles $p_{2,3}$ are not dependent on the low-pass filter but only on the gains of the PI controller.

Therefore, as it can be seen by increasing the bandwidth of the low-pass filter, the real pole is moved way out in the left-half plane giving a fast response of the system.

By introducing the feed-forward term to the linear SRF-PLL, the open-loop transfer function where the SRF-PLL is tuned with a bandwidth of 10 Hz and a first and a second order low-pass filter in the feed-forward path with a bandwidth of 100 Hz is presented in Fig. 4.

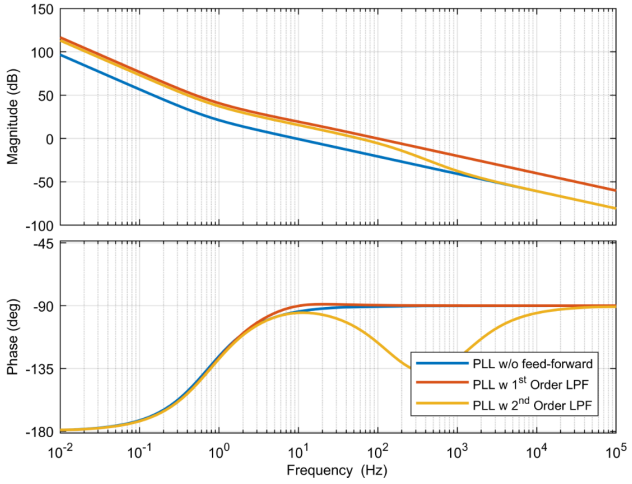

Fig. 4. Open-loop transfer function of the linear SRF-PLL with and without feed-forward control.

Here it is evident that a high gain is introduced at in a higher frequency range using the feed-forward control which improves its high-frequency dynamic response. The phase margin of the two are identical and is $\phi_m = 85.5°$ which is introduced by the slow inner SRF-PLL. Since the phase increases as the frequency increase the gain margin of the system with and without feed-forward control is -34.5 dB and -∞ dB, respectively. Since the frequency is increasing, a negative gain margin simply means that the gain can be lowered by the mentioned amount without loosing stability.

As it can be seen in Fig. 5, by using phase angle error feed-forward a stable response with a significantly increased bandwidth can be achieved with a first order low-pass filter. In Fig. 5 the bandwidth of the first order low-pass filter matches exactly the bandwidth of the closed-loop system, i.e. 100 Hz for this design. The same dynamic response can be achieved with a SRF-PLL and the a bandwidth of 100 Hz, so there is no further increase neither in dynamics nor stability by only using a first order LPF. Additional controls can still be included to enhance the performance. This is further shown in Section III-B.

Nevertheless, with a second order low-pass filter is it possible to achieve a higher bandwidth, but higher frequencies are controlled as with a slow tuned SRF-PLL. A trade-off between bandwidth and stability can be achieved with optimized tuning of the second order filter.

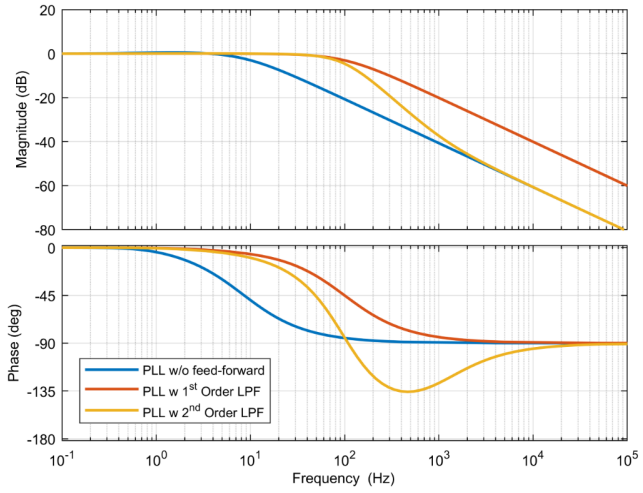

Fig. 5. Closed-loop transfer function of the linear SRF-PLL with and without feed-forward control.

Design Guideline:

The SRF-PLL can be tuned to give a desired damping ratio and natural frequency based on the general second order system shown in (7). When this is done, the bandwidth of the low-pass filter can be increased to improve the dynamic response of the overall system. However, it should be noticed that ignoring the effect of the inner current controller and digital delays will only be valid for $\alpha_F \ll \alpha_c$ where α_c is the bandwidth of the inner current regulator. Therefore, α_F should be tuned dependent on system and network parameters and it is recommended to select $\alpha_F < f_s/50$ where f_s is the sampling frequency of the control system. This is to make sure the synchronization loop is kept sufficiently slower than the inner current loop. In this way, a fast synchronization unit can be achieved a fast dynamic response but the inner SRF-PLL can be designed with a low bandwidth (<10 Hz) to limit the steady-state frequency oscillations.

B. Feed-Forward

This Section will further describe some of the possibilities to design the feed-forward block shown in Fig. 2.

In Fig. 6 a phase jump of 60° is performed to visualize the input/outputs of the proposed controller presented in Fig. 2. The processing in the feed-forward is a low-pass filter with a cutoff frequency of 100 Hz. As it can be seen, a filtered signal of the angle deviation is used to seamlessly track the phase jump within 5 ms.

As it can be seen in Fig. 6 the feed-forward term is following the error signal with some delay, that is inherent in the low-pass filter. The delay will cause a over-compensation of the error signal in the feed-forward. This can be compensated by a reduction of the gain of the LPF. The gain reduction and the effect on the feed-forward value can be seen in Fig. 7.

Besides filtering, the error signal can also be limited in value or in rate of change. Furthermore, the controller structure makes it also possible to use a dead-band to decide, based on the angle error signal, whether the proposed

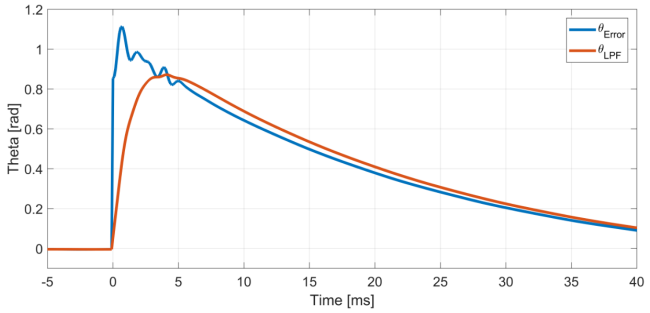

Fig. 6. Feed-forward Function with a low-pass filter during a 60° phase jump.

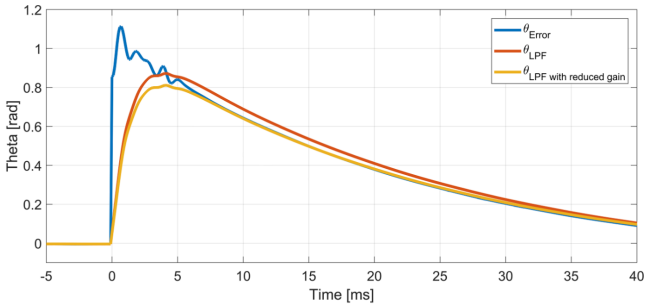

Fig. 7. Feed-forward Function with a low-pass filter with reduced gain during a 60° phase jump.

feed-forward should be activated, or not.

One way to smoothly enable and disable the feed-forward signal is e.g. to use deadband and then a LPF. This allows the decoupling of the feed-forward during the steady state. There will be no influence to the synchronization, if the angle deviation does not exceed the threshold. Only during transient events will be a coupling and the controller interactions are limited to these events. This can especially be helpful under low voltage conditions, where the fast angle signal in highly dependent on the converter output itself.

In the simulations shown in Fig. 8 is a dead-band together with a low-pass filter used. The dead-band is set to reduce angle deviations, that are lower than 10° in this case. This combination allows a fast angle deviation tracking when there are severe angle deviations, but also a robustness against low magnitude angle deviations, that are caused by harmonics or measurement uncertainties. This low deviation robustness can be seen after 28 ms in the simulation results. In this case, the feed-forward is decoupled from the synchronization.

Hence this control structure can be adapted and tailored for any performance criteria of interest. If the angle difference is not processed at all, then the controller will react as an ideal angle control with the fastest response possible.

IV. Verification of Proposed Controller

In this section, the operation of the proposed controller is presented with simulation and experimental results. For the

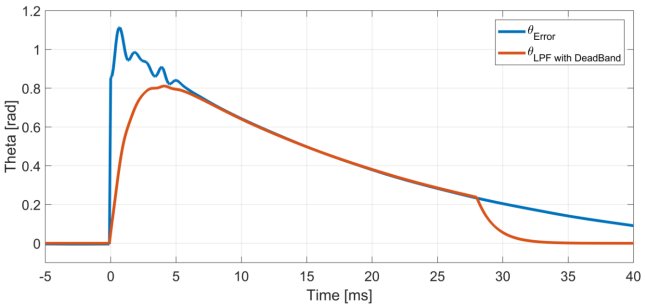

Fig. 8. Feed-forward Function with a low-pass filter and a dead-band during a 60° phase jump.

results to be presented, the feed-forward block is realized as a first order LPF with a cut-off frequency of 100 Hz, which was found to give a smooth but still fast response.

A. Simulation Results

The proposed controller is subjected to two simulation tests, performed with the simulation software EMTDC / PSCAD. At first, the synchronization is tested during a 60° phase jump to reveal the performance of the controller dynamics. Secondly, the synchronization is tested during a symmetrical three-phase fault including a 60° phase jump and a drop of the voltage to 0.2 pu.

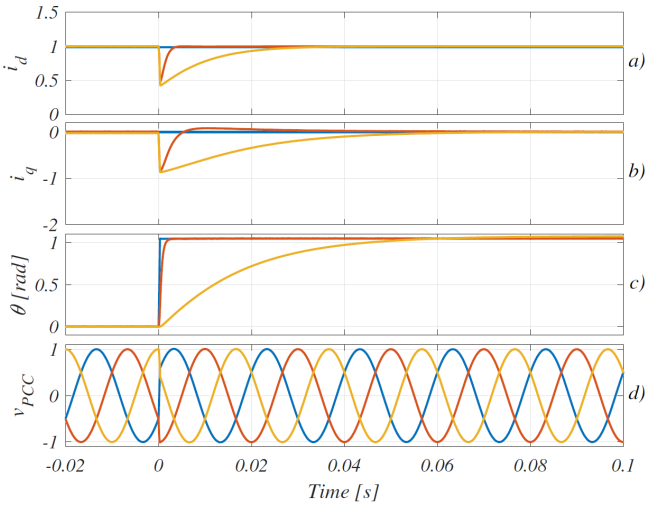

Fig. 9. Comparison of SRF-PLL and the proposed controller during a 60° phase jump in the abc grid voltages.
In subfigures a), b) and c), yellow is SRF-PLL and red is proposed method. Blue in subfigures a) and b) is the reference value of the current. Blue in subfigure c) is the angle estimation with an ideal angle calculation.

Fig. 9 shows the controller behavior during a phase jump occurring at 0 sec. As anticipated, the proposed method greatly enhances the dynamic performance of the synchronization and it is able to track the phase jump within 5 ms, whereas the SRF-PLL takes around two fundamental cycles to track the changed grid voltage angle.

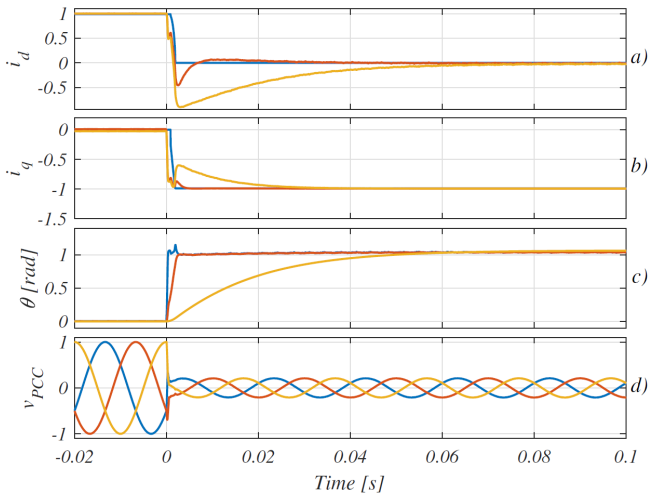

Fig. 10. Comparison of SRF-PLL and the proposed controller during a severe three-phase symmetrical fault.
In subfigures a), b) and c), yellow is SRF-PLL and red is proposed method. Blue in subfigures a) and b) is the reference value of the current. Blue in subfigure c) is the angle estimation with an ideal angle calculation.

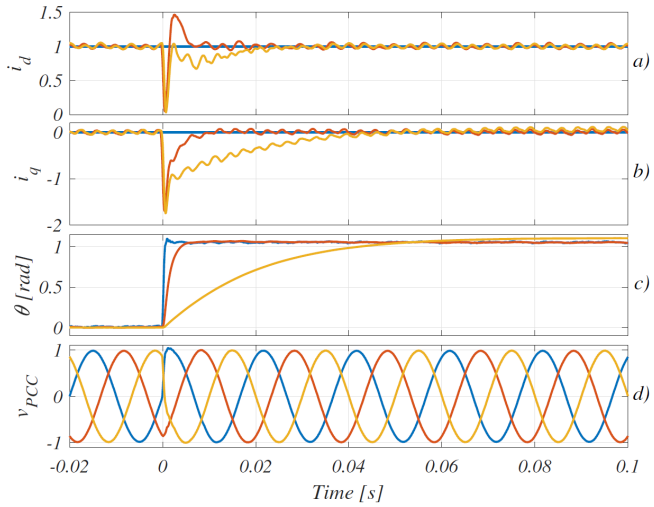

Fig. 11. Comparison of SRF-PLL and the proposed controller during a 60° phase jump in the abc grid voltages.
In subfigures a), b) and c), yellow is SRF-PLL and red is proposed method. Blue in subfigures a) and b) is the reference value of the current. Blue in subfigure c) is the angle estimation with an ideal angle calculation.

Fig. 10 shows the synchronization process for a severe three-phase fault with a 60° phase jump. Again a large improvement in the transient response is evident and the proposed controller is almost able to keep the reversed active power flow from occurring. Looking at the response for the SRF-PLL, reversed active power flow is happening for two fundamental cycles, which is not acceptable according to grid codes and also inconvenient for the converter itself.

B. Experimental Results

The proposed synchronization unit is tested on a laboratory setup consisting of a three-phase two-level VSC connected to a grid simulator through an inductive impedance for validation of the simulation results. The grid-connected converter is equipped with an LCL-filter on the output and the converter regulates the converter side currents using proportional resonant controllers implemented in $\alpha\,\beta$ - frame.

Similarly as shown for the simulations, two tests were performed, a 60° phase jump during normal operating conditions and a symmetrical three-phase fault with a 60° phase jump and 0.2 pu grid voltage.

Fig. 11 shows a comparison between the proposed method and SRF-PLL during a phase jump. As it can be seen, the proposed controller is able to track the phase of the grid voltage within 5 ms, whereas the slow SRF-PLL takes several fundamental cycles to do so. This makes it possible to quickly regulate the reactive current to return to zero. An overshoot is present in the d-axis current, which is anticipated to be due to improper tuning of the current controller, which is not the focus of this paper.

Fig. 12 illustrates the response for a symmetrical three-phase fault including a 60° phase jump. As demonstrated before, the proposed method quickly tracks the phase jump, which

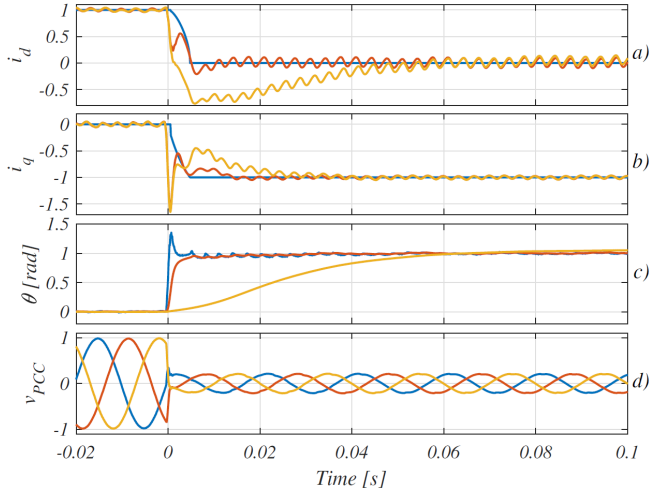

Fig. 12. Comparison of SRF-PLL and the proposed controller during a severe three-phase symmetrical fault.
In subfigures a), b) and c), yellow is SRF-PLL and red is proposed method. Blue in subfigures a) and b) is the reference value of the current. Blue in subfigure c) is the angle estimation with an ideal angle calculation.

allows the current controller to regulate the active and reactive currents to their reference values within the requirements set by the grid codes. As it can be seen for the case of SRF-PLL, reversed active power flow is observed for several cycles, which is highly undesired during such conditions due to the power being accumulated on the DC-side of the grid-connected converter.

V. Conclusions

Fast and accurate synchronization capability of grid-connected converters is particularly important to ensure proper

performance during transient events, such as grid faults. In this paper, a synchronization method which significantly improves the dynamic performance of the phase tracking capability of the SRF-PLL has been proposed. This is achieved by combining a conventional SRF-PLL with a fast feed-forward path based on an ideal angle estimation. The advantages of this method are twofold:

1: The linear SRF-PLL can be tuned with a low bandwidth to ensure robust small-signal performance with low steady-state variations.

2: The feed-forward angle compensation allows an additional level of control, which can be designed in many different ways to achieve desired transient dynamics of the synchronization process.

The proposed controller were subjected to phase jumps and three-phase fault during a simulation study which were validated experimentally.

REFERENCES

[1] E. Afshari, G. R. Moradi, R. Rahimi, B. Farhangi, Y. Yang, F. Blaabjerg, and S. Farhangi, "Control Strategy for Three-Phase Grid-Connected PV Inverters Enabling Current Limitation Under Unbalanced Faults," *IEEE Transactions on Industrial Electronics*, vol. 64, no. 11, pp. 8908–8918, Nov 2017.

[2] M. Abdelrahem and R. Kennel, "Direct-Model Predictive Control for Fault Ride-Through Capability Enhancement of DFIG," in *PCIM Europe 2017; International Exhibition and Conference for Power Electronics, Intelligent Motion, Renewable Energy and Energy Management*, May 2017, pp. 1–8.

[3] R. Teodorescu, M. Liserre, and P. Rodriguez, *Grid Converters for Photovoltaic and Wind Power Systems*. John Wiley & Sons, 2011, vol. 29.

[4] S. Golestan, J. M. Guerrero, and J. C. Vasquez, "Three-Phase PLLs: A Review of Recent Advances," *IEEE Transactions on Power Electronics*, vol. 32, no. 3, pp. 1894–1907, March 2017.

[5] F. Blaabjerg, R. Teodorescu, M. Liserre, and A. V. Timbus, "Overview of Control and Grid Synchronization for Distributed Power Generation Systems," *IEEE Transactions on Industrial Electronics*, vol. 53, no. 5, pp. 1398–1409, Oct 2006.

[6] D. Dong, B. Wen, D. Boroyevich, P. Mattavelli, and Y. Xue, "Analysis of Phase-Locked Loop Low-Frequency Stability in Three-Phase Grid-Connected Power Converters Considering Impedance Interactions," *IEEE Transactions on Industrial Electronics*, vol. 62, no. 1, pp. 310–321, Jan 2015.

[7] B. H. Kim and S. K. Sul, "Stability-Oriented Design of Frequency Drift Anti-Islanding and Phase-Locked Loop Under Weak Grid," *IEEE Journal of Emerging and Selected Topics in Power Electronics*, vol. 5, no. 2, pp. 760–774, June 2017.

[8] S. Ma, H. Geng, L. Liu, G. Yang, and B. C. Pal, "Grid-Synchronization Stability Improvement of Large Scale Wind Farm During Severe Grid Fault," *IEEE Transactions on Power Systems*, vol. 33, no. 1, pp. 216–226, Jan 2018.

[9] Ö. Göksu, "Control of Wind Turbines during Symmetrical and Asymmetrical Grid Faults," Ph.D. dissertation, Aalborg University, 2012.

[10] BDEW. (1999) Technical Guideline: Generating Plants Connected to the Medium Voltage Network. [Online]. Available: http://www.bdew.de

[11] H. A. Hamed, A. F. Abdou, E. H. E. Bayoumi, and E. E. EL-Kholy, "A Fast Recovery Technique for Grid-Connected Converters After Short Dips Using a Hybrid Structure PLL," *IEEE Transactions on Industrial Electronics*, vol. 65, no. 4, pp. 3056–3068, April 2018.

[12] C. Subramanian and R. Kanagaraj, "Rapid Tracking of Grid Variables Using Prefiltered Synchronous Reference Frame PLL," *IEEE Transactions on Instrumentation and Measurement*, vol. 64, no. 7, pp. 1826–1836, July 2015.

[13] H. A. Hamed, A. F. Abdou, E. E. El-Kholy, and E. H. E. Bayoumi, "Adaptive Cascaded Delayed Signal Cancelation PLL Based Fuzzy Controller Under Grid Disturbances," in *2016 IEEE 59th International Midwest Symposium on Circuits and Systems*, Oct 2016, pp. 1–4.

[14] R. H. Park, "Two-Reaction Theory of Synchronous Machines Generalized Method of Analysis - Part I," *Transactions of the American Institute of Electrical Engineers*, vol. 48, no. 3, pp. 716–727, July 1929.

[15] R. Teodorescu and F. Blaabjerg, "Flexible Control of Small Wind Turbines With Grid Failure Detection Operating in Stand-Alone and Grid-Connected Mode," *IEEE Transactions on Power Electronics*, vol. 19, no. 5, pp. 1323–1332, Sept 2004.

[16] I. Serban and C. Marinescu, "Control Strategy of Three-Phase Battery Energy Storage Systems for Frequency Support in Microgrids and with Uninterrupted Supply of Local Loads," *IEEE Transactions on Power Electronics*, vol. 29, no. 9, pp. 5010–5020, Sept 2014.

[17] F. Liccardo, P. Marino, and G. Raimondo, "Robust and Fast Three-Phase PLL Tracking System," *IEEE Transactions on Industrial Electronics*, vol. 58, no. 1, pp. 221–231, Jan 2011.